Wave energy extraction by coupled resonant absorbers

By D.V. Evans and R. Porter

School of Mathematics, University of Bristol, Bristol BS8 1TW, UK.

In this article a range of problems and theories will be introduced which will build towards a new wave energy converter (WEC) concept with the acronym 'ROTA' standing for Resonant Over-Topping Absorber. First, classical results for wave power absorption for WECs constrained to operate in a single degree of freedom will be reviewed and the role of resonance in their operation highlighted. Emphasis will then be placed on how the introduction of further resonances can improve power take-off characteristics by extending the range of frequencies over which the efficiency is close to a theoretical maximum. Methods for doing this in different types of WECs will be demonstrated. Coupled resonant absorbers achieve this by connecting a WEC device equipped with its own resonance (determined from a hydrodynamic analysis) to a new system having separate mass/spring/damper characteristics. It is shown that a coupled resonant effect can be realised by inserting a water tank into a WEC and this idea forms the basis of the ROTA device. In essence the idea is to exploit the coupling between the natural sloshing frequencies of the water in the internal tank and the natural resonance of a submerged buoyant circular cylinder device which is tethered to the sea floor allowing a rotary motion about its axis of attachment.

Keywords: Efficiency, Capture width, Multi-resonance, Coupled resonance, Sloshing

1. Introduction

The quadrupling of the price of oil in the mid-1970s led the UK government to initiate a major research and development programme aimed at establishing the feasibility of extracting useful electrical energy from ocean waves and to estimate the cost of this energy if used on a large-scale to supply UK needs. This was quickly followed by smaller programmes in Japan, Scandinavia, Portugal and the USA. The programme ran from 1974 to 1983 and a large number of ideas for capturing wave energy were considered. The most promising of these were tested at small scale in wave tanks with three devices being tested in sea conditions at one-tenth scale. Towards the end of the programme eight device teams drawn from universities, government research establishments and industry in the UK had produced and costed reference designs for a 2GW wave power station located off NW Scotland. In 1982 the Department of Energy concluded that the overall economic prospects for wave energy looked poor when compared with other electricity-producing renewable energy technologies and the programme was terminated apart from some small-scale generic research.

More recently, concerns over global warming have prompted a revival of interest in wave energy with the UK taking a leading role. Thus there have been significant investments from the UK government through Research Councils and other initiatives such as the SUPERGEN marine energy consortium led by Edinburgh University, the Marine Renewables Proving Fund (MRPF), the Energy Technologies Institute (ETI) and the Technology Strategy Board (TSB) to fund industry and University partnerships in developing commercially-viable wave energy converters (WECs). Examples of WECs developed under these schemes include the Pelamis WEC and the Oyster 2.

Much of the early theoretical work on WECs concentrated on estimating the maximum power a particular device could absorb using classical linear water wave theory. Despite the limitations of this theory many interesting and useful results were derived and confirmed by small scale tank tests. Although some background theoretical work continues, much of the current focus of WEC development has been on numerical modelling using software such as WAMIT, ANSYS/CFX and SPH-based code together with experimental wave tank tests leading to, in a small number of cases, the testing of prototypes in open waters. Excellent reviews of the current state of theoretical, numerical and experimental modelling of WECs can be found in Falnes (2002), Cruz (2008) and Falcão (2010).

Many WECs utilise resonance of one kind or another to achieve high levels of power absorption and for a generic WEC in the form of a rigid body operating in a single degree of freedom the theory is well-known. Less is known about multi-resonant devices where the possibility of widening the bandwidth of the power absorption curve as a function of frequency exists. It is such devices on which the present paper is focussed.

We begin in the next section by summarizing the existing theory for WECs operating in a single mode of motion in the case of a rigid body motion moving against a fixed reference and show how power output is maximised by impedance matching; that is, by simultaneously balancing the inertia and restoring forces so that the system is in resonance, whilst matching the radiation damping of the WEC with the externally imposed damping. We also consider a simple example of an oscillating water column (OWC) device and derive similar expressions for the power absorbed in which the exciting force and velocity in the rigid body case are simply replaced by the mean volume flux across, and the surface pressure on, the internal free surface of the OWC respectively. We point out important differences between the two types of devices in terms of the resonances which can arise. The main section of the paper is §3 where we consider examples of *coupled resonant systems*. We begin with a simple double-body device in which the rigid body exposed to the waves moves against another body either internal or external to the first which is also free to move, with power being taken off through the relative motion between them. The second example is of an axisymmetric doubly-resonant OWC in which there are two water columns each with its own resonant properties. A third example relates to devices with projecting side-walls where an additional resonance is created which can enhance the wave amplitude reaching the device. A novel example follows in which we consider the coupling of the motion of a rigid body WEC to the sloshing motion of an internal body of water. Expressions are obtained for the power absorbed through a turbine positioned in the enclosed air space above the internal free surface. In a final section a description is given of

the ROTA, standing for Resonant Over-Topping Absorber, a practical device based on the previous idea but where the power take off involves the overtopping of the internal fluid into an inner reservoir which then feeds a low-head turbine.

2. A brief review of wave energy theory

(*a*) *A single mode rigid body motion*

We consider for clarity and simplicity a simple WEC oscillating in regular waves of frequency $\omega/2\pi$ in a single degree of freedom. Examples include an axisymmetric buoy constrained to oscillate in heave and subject to its natural hydrostatic restoring force or a truncated buoyant closed circular cylinder, totally submerged with its axis horizontal, and tethered to the sea bed by inextensible mooring lines from each end, which oscillates in pitch in response to the component of the tension in the moorings due to the its buoyancy. This device could also span a narrow wave tank in which case the problem may be regarded as two-dimensional with quantities referring to unit length across of the tank. For additional clarity throughout the paper we shall use expressions based on the assumption of infinite water depth. The modifications required in places for finite depth involve a factor given by Falnes (2002, p.69, eqn 4.80) and Newman (1976, eq.18) which is close to unity in all the illustrative examples involving finite depth.

In considering the equations of motion, it is convenient to extract the time dependence so that a quantity F is understood to mean the time independent form of f=Re$\{F\mathrm{e}^{-\mathrm{i}\omega t}\}$.

In what follows the terms force, velocity and mass should be interpreted as couple, angular velocity and moment of inertia according to the example to which it applies. Thus we have as the equation of motion of the WEC,

$$X_e + X_w - \mathrm{i}\omega^{-1}CU = -\mathrm{i}\omega MU. \tag{2.1}$$

Here, X_e is the external force acting on the device (this could by provided through a mechanism for power absorption, for example), X_w is the external force on the device due to the waves, C is a constant arising from any restoring force, hydrostatic or otherwise, assumed to be proportional to and opposed to the device displacement $\mathrm{i}\omega^{-1}U$, where U is the velocity of the device, $-\mathrm{i}\omega U$ its acceleration, and M is its mass. It is traditional to decompose X_w as

$$X_w = (\mathrm{i}\omega A - B)U + X_s, \tag{2.2}$$

where the first term on the right-hand side is the force induced on the device due to its own motion and proportional to its velocity, U, expressed in terms of A, B, the *added mass* and *radiation damping* coefficients (respectively) for the device, each dependent on frequency. The second term, X_s, is the exciting force due to the waves on the device, when assumed fixed, also a function of frequency. It follows from equations (2.1), (2.2), that

$$UZ = X_s + X_e, \tag{2.3}$$

where

$$Z \equiv B - \mathrm{i}\omega(M + A - \omega^{-2}C). \tag{2.4}$$

The *mean power*, W, generated by the wave forces on the device is the time average over a period, $2\pi/\omega$, of the product of those waves forces and the device velocity which reduces to

$$W = \tfrac{1}{2}\,\mathrm{Re}\{X_w\overline{U}\} = \tfrac{1}{2}\,\mathrm{Re}\{X_s\overline{U}\} - \tfrac{1}{2}B|U|^2, \tag{2.5}$$

(the overbar denoting complex conjugation) from (2.2), which can be re-arranged as

$$W = \frac{1}{8}\frac{|X_s|^2}{B} - \frac{1}{2}B\left|U - \frac{X_s}{2B}\right|^2, \tag{2.6}$$

provided $B \neq 0$. It follows that the maximum mean power achievable is given by

$$W_{max} = \frac{1}{8}\frac{|X_s|^2}{B}, \tag{2.7}$$

and occurs when the velocity, U, equals $X_s/2B$. Notice from (2.6) that no mean power is absorbed if either $U = 0$ (obviously) or $U = X_s/B$ (less obviously). Notice also that in both cases U is in phase with the exciting force. So, regardless of the precise form of the external force on the device we have determined the maximum available mean power. In two dimensions (e.g. a device of constant cross-section spanning a wave tank under normally-incident waves from $x = -\infty$) the quantities X_s and B are connected by the formula (see, for example, Newman (1976))

$$|X_s|^2/B = 8W_{inc}\gamma, \tag{2.8}$$

where W_{inc} is the mean power incident per unit crest length, and

$$\gamma = |A_-|^2/(|A_+|^2 + |A_-|^2), \tag{2.9}$$

where A_+, A_- are the complex wave amplitudes of the waves generated towards $x = +\infty$ and $x = -\infty$ (respectively) by the forced motion of the device in the absence of incident waves. Thus, in two dimensions, we may define an *efficiency of absorption* $E \equiv W/W_{inc}$ having a maximum defined as

$$E_{max} = W_{max}/W_{inc} \equiv \gamma, \tag{2.10}$$

a result first obtained independently by Mei (1976), Evans (1976) and Newman (1976). This formula helps to explain the high efficiency of the Salter duck (Salter, 1974) whose shape is such that $|A_+| \ll |A_-|$.

For a three dimensional device we define a *capture width* l by

$$l \equiv W/W_{inc}, \tag{2.11}$$

which represents the equivalent length of incident wave from which all power is taken. For an axisymmetric device oscillating in heave it is known (Newman 1976) that

$$2\pi|X_s|^2 = 8BLW_{inc}, \tag{2.12}$$

where L represents the incident wavelength henceforth, so that it follows from (2.7) that

$$l_{max} = W_{max}/W_{inc} = L/2\pi, \tag{2.13}$$

a result first proved independently by Budal & Falnes (1975), Evans (1976) and Newman (1976). Remarkably, this result demonstrates that the maximum theoretical capture width is independent of the physical dimensions of the device, provided the incident wave amplitude is below a certain value.

(*b*) *Motion against a fixed reference*

In the usual theory for wave energy devices, it is assumed that the device moves against a fixed reference providing a mechanism for power take-off and that

$$X_e = -\lambda U, \tag{2.14}$$

where, in general, $\lambda = d + \mathrm{i}\omega^{-1}\kappa$ with d a positive damping constant and κ is a spring constant, which could be zero. It follows from (2.3), (2.14) that

$$U(\lambda + Z) = X_s. \tag{2.15}$$

Now the mean power absorbed by the device is calculated by

$$W = -\tfrac{1}{2}\,\mathrm{Re}\{X_e\overline{U}\} = \tfrac{1}{2}d|U|^2, \tag{2.16}$$

using (2.14) so that, in the two-dimensional case, the efficiency is defined as

$$E \equiv W/W_{inc} = \frac{4dB\gamma}{|\lambda + Z|^2}, \tag{2.17}$$

from (2.8), (2.15). A short calculation shows that

$$\frac{2d}{|\lambda + Z|^2} = \frac{\lambda + \overline{\lambda}}{|\lambda + Z|^2} \equiv \frac{1}{2\,\mathrm{Re}\{Z\}}\left(1 - \frac{|\lambda - \overline{Z}|^2}{|\lambda + Z|^2}\right), \tag{2.18}$$

so that

$$E = \gamma\left(1 - \frac{|\lambda - \overline{Z}|^2}{|\lambda + Z|^2}\right). \tag{2.19}$$

It follows that

$$E_{max} = \gamma, \tag{2.20}$$

in agreement with (2.10). This maximum efficiency is achieved when $\lambda = \overline{Z}$ implying that

$$d = B(\omega), \quad \text{and} \quad \kappa/\omega^2 = M + A(\omega) - C/\omega^2, \tag{2.21}$$

must be satisfied simultaneously for a given value of ω. In practice λ is often real in which case we return to (2.17) and use the identity

$$\frac{\lambda}{|\lambda + Z|^2} = \left(1 - \frac{(\lambda - |Z|)^2}{|\lambda + Z|^2}\right)\frac{1}{2(|Z| + \mathrm{Re}\{Z\})}, \tag{2.22}$$

from which it follows that

$$E_{max} = \left(\frac{2B}{|Z| + B}\right)\gamma, \tag{2.23}$$

achieved when $\lambda = |Z|$.

The corresponding result for the axisymmetric device in heave is obtained by using (2.11), (2.12), (2.15) and (2.16) to obtain the capture width

$$l = \frac{2dBL}{\pi|\lambda + Z|^2}, \tag{2.24}$$

so that

$$l_{max} = L/2\pi, \tag{2.25}$$

achieved when $\lambda = \overline{Z}$ in agreement with (2.13), and

$$l_{max} = \left(\frac{2B}{|Z| + B}\right) L/2\pi, \tag{2.26}$$

when $\lambda = |Z|$ and is real.

Consider the results (2.23) and (2.26) with λ assumed real. Then it is clear that the maximum mean power arises when $|Z|$ is a minimum or when $D \equiv \mathrm{Im}\{Z\} = M + A - C/\omega^2 = 0$ which corresponds to resonance of the system. In general, for a single heaving rigid body, $A(\omega)$ and $B(\omega)$ vary smoothly with increasing ω with A having a single maximum and B monotonically decreasing. Thus $D = 0$ for just one value of ω and the system has a single resonant frequency.

(i) *An illustrative example*

We consider power absorption from a two-dimensional WEC device consisting of a semi-submerged horizontal circular cylinder of radius a which is free to move in heave in response to the incident waves. The power take-off is effected by a piston driven by vertical rod connected to the cylinder. Thus, in this example, $\lambda = d$ and the spring constant $\kappa = 0$ whilst the fore-aft symmetry of the cylinder implies $A_- = A_+$ and hence $\gamma = \frac{1}{2}$. That is, the efficiency, E, given by (2.20), of this device can never exceed $\frac{1}{2}$. Since λ is real, the maximum efficiency, E_{max} is given by (2.23) and $E_{max} = \frac{1}{2}$ only when $\lambda = \overline{Z}$ or, equivalently, when $d = B$ and $M + A(\omega) - C/\omega^2 = 0$.

In this example, $C = 2a\rho g$, represents the hydrostatic restoring force on the cylinder where ρ is the density of the fluid, $M = \frac{1}{2}\rho\pi a^2$ is the mass (by Archimedes' principle), whilst $A(\omega)$, $B(\omega)$ are the heave added mass and radiation damping coefficients, computed using the methods outlined in Martin & Dixon (1983), for example. Non-dimensional coefficients $\mu = A/M$ and $\nu = B/(M\omega)$ are defined, whilst a non-dimensional damping constant is defined with $\hat{d} = d(a/g)^{1/2}/M$ such that $\lambda/(M\omega) = \hat{d}/(Ka)^{1/2}$ where $Ka \equiv \omega^2 a/g$

In figure 1 the dashed curve shows the variation of E_{max} with Ka, peaking at $\frac{1}{2}$ when $M + A(\omega) - C/\omega^2 = 0$ (or $1 + \mu - 4/(\pi Ka) = 0$ in terms of non-dimensional quantities). The solid curves show how different choices of fixed damping constant, $\hat{d}$, affect the efficiency across a range of frequencies, each curve never able to exceed the curve of E_{max}. Figure 2 shows the associated variation of μ and ν with Ka as well as the variation of D, which crosses zero at just one frequency given by $Ka \approx 0.797$ where $\nu \approx 0.523$. Thus, to achieve the maximum efficiency of $\frac{1}{2}$ here, $\hat{d} = \nu(Ka)^{1/2} \approx 0.467$. The curve of $\hat{d} = \frac{1}{2}$ is close to this value and hence the high peak efficiency associated with $\hat{d} = \frac{1}{2}$ in figure 2. We observe that for $\hat{d} < 0.467$, E never obtains its maximum E_{max}, whilst for $\hat{d} > 0.467$, E equals E_{max} (where it is required that $\lambda = |Z|$) at two separate frequencies. Beyond $Ka = 2$, the curves all tend to zero with no further peaks.

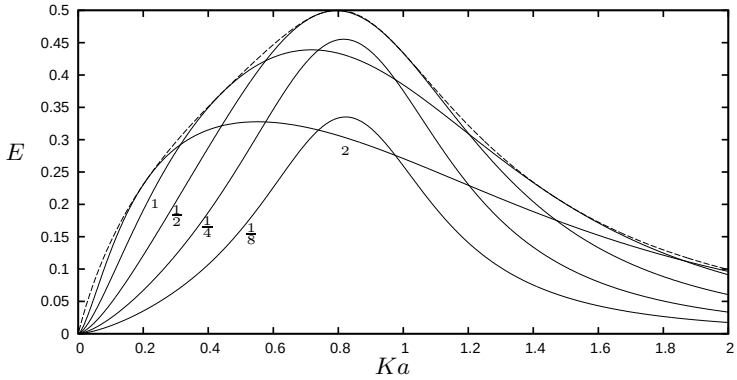

Figure 1. Curves showing efficiency, E, against Ka for a heaving semi-immersed horizontal cylindrical buoy WEC, radius a, with fixed dimensionless damping constants, $\hat{d}$ (shown against curves), from $\frac{1}{8}$ to 2. The thick dashed curve is $E = E_{max}$.

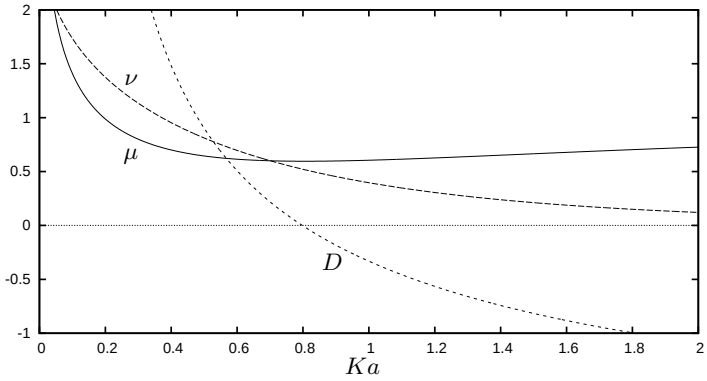

Figure 2. Dimensionless added mass μ and radiation damping ν and D against $Ka \equiv \omega^2 a/g$.

(*c*) *Oscillating water column devices*

The simplest example of an oscillating water column (OWC) device is a fixed vertical partially-immersed thin-walled circular cylindrical tube open at its lower end and constricted at its upper end above the internal free surface by an opening housing an air-turbine. The oscillatory pressure at the lower end due to the incident waves causes the column of water inside the tube to oscillate and force the air above the internal free surface through a bi-directional air turbine (the Well's turbine being most commonly used). It is a simple matter to show that for tubes that are narrow (relative to L, the incident wavelength and ℓ, the draft of the tube) the column of water of length ℓ inside the tube will behave like a rigid body and will resonate at a radian frequency given by $(g/\ell)^{1/2}$. The theory of the last section can easily be adapted to estimate the power absorbed by such a system when the external structure has an arbitrary shape. As in the previous section, a time-dependence has been factored from quantities of interest. Thus the total volume

flux across the internal free surface due to the incident waves can be written

$$Q_w = Q_s + (\mathrm{i}\omega D - B)P, \tag{2.27}$$

where P is the dynamic air pressure (relative to atmospheric pressure) on the internal free surface, Q_s is the volume flux across the internal free surface when P is taken to be zero, corresponding to an internal free surface open to the atmosphere, and the second term on the right-hand-side is the volume flux across the free surface due to the induced pressure, P, acting upon it. Here D and B are coefficients dependent only on ω termed the *radiation susceptance* and *radiation conductance* respectively by Falnes (2002, p.229). They play a role in OWC devices similar to the added mass and radiation damping terms for the rigid body theory of §2 *b* but we shall see there is a fundamental difference in their dependence on ω.

Now the mean power absorbed is by this system is

$$W = \tfrac{1}{2}\,\mathrm{Re}\{Q_w\overline{P}\} = \tfrac{1}{2}\,\mathrm{Re}\{Q_s\overline{P}\} - \tfrac{1}{2}B|P|^2, \tag{2.28}$$

from (2.27), which can be re-arranged as

$$W = \frac{1}{8}\frac{|Q_s|^2}{B} - \frac{1}{2}B\left|P - \frac{Q_s}{2B}\right|^2, \tag{2.29}$$

provided $B \neq 0$. It follows that the maximum mean power achievable is given by

$$W_{max} = \frac{1}{8}\frac{|Q_s|^2}{B}. \tag{2.30}$$

Notice the similarity with the rigid body case with force and velocity being replaced by volume flux and free surface pressure respectively. The flow through the turbine can be modelled by a linear relation between the volume flux and the pressure. Thus we assume

$$Q_w = \lambda P, \tag{2.31}$$

where $\lambda = d + \mathrm{i}\omega^{-1}\kappa$ with d a positive damping coefficient and κ models the air compressibility. It follows from (2.27), (2.31) that

$$P(\lambda + Z) = Q_s, \tag{2.32}$$

where the previous definition of Z used in §2 *b* is replaced here with

$$Z \equiv B - \mathrm{i}\omega D. \tag{2.33}$$

Now the mean power developed by the turbine is,

$$W = \tfrac{1}{2}\,\mathrm{Re}\{Q_w\overline{P}\} = \tfrac{1}{2}d|P|^2, \tag{2.34}$$

so that

$$W = \frac{|Q_s|^2 d}{2|\lambda + Z|^2}, \tag{2.35}$$

from (2.32). We now proceed as for the rigid body case to obtain the result (2.30), achieved when $\lambda = \overline{Z}$ or $d = B$ and $\kappa/\omega^2 = D$.

If we neglect compressibility (as is often done) and assume λ is real then as in the rigid body case we obtain

$$W_{max} = \frac{|Q_s|^2}{4(|Z| + B)}, \tag{2.36}$$

achieved when $\lambda = |Z|$. It can be shown, (Evans 1982) that in two dimensions the quantities Q_s and B are connected by the formula

$$|Q_s|^2/B = 8W_{inc}\gamma, \tag{2.37}$$

and for a three-dimensional axisymmetric device absorbing in heave that

$$2\pi|Q_s|^2 = 8BLW_{inc}. \tag{2.38}$$

It follows that equations (2.20), (2.26) derived from rigid body motions are valid for OWCs also with the new definitions of Z and B.

It is clear that the theories for rigid body and OWC devices are similar with the radiation damping B being replaced by the radiation conductance B and the inertia terms $D \equiv M + A - C/\omega^2$ involving the added mass A and hydrostatic restoring force C being replaced by the radiation susceptance D. In both cases when λ is real then maximum power requires $D = 0$ as the resonance condition. As we have seen in the case of a rigid body WEC this condition is generally satisfied by a single value of frequency, say, ω_0 so that the power absorbed peaks at this frequency and falls off on either side. See for example Evans *et al.* (1979) where both theoretical and experimental results for the efficiency of power absorption by the Bristol Cylinder device are presented. This is not the case with the radiation susceptance as is illustrated in figure 3 below (where μ is the non-dimensional equivalent of D) for a generic three-dimensional OWC device. Also see figure 2 from Evans & Porter (1995) for similar curves in a two-dimensional OWC device. Thus the susceptance is seen to have a number of zeros which can affect the performance of the device by increasing the peaks in power output as reference to the formula

$$l_{max} = \left(\frac{2B}{|Z| + B}\right) L/2\pi, \tag{2.39}$$

shows since at a zero $|Z| = B$. Also see Falnes (2002, p.231).

(i) *An illustrative example*

We consider the problem of a three-dimensional OWC device consisting of an open-ended thin-walled tube immersed to a depth ℓ in water of finite depth h. The radius of the tube is given by b. Air is pumped through a turbine connecting the air-space above the internal water surface with the atmosphere. Effects of compressibility are ignored and so we take $\lambda = d$, where d is the turbine damping coefficient through which power is extracted. As in the previous section, some non-dimensionalisation is required and here we define dimensionless quantities $\mu = \rho g D/(\pi b^2)$ and $\nu = \rho g B/(\omega \pi b^2)$. In addition, we define $\hat{d} = d(g/\ell)^{1/2}/(\pi b^2)$ as a dimensionless damping coefficient so that $\lambda/(\omega\pi b^2) \equiv \hat{d}/(K\ell)^{1/2}$.

Figure 3 illustrates the variation of the two key coefficients μ and ν with $Kb \equiv \omega^2 b/g$. In this example, where $b/\ell = 8$ and the diameter of the OWC is large

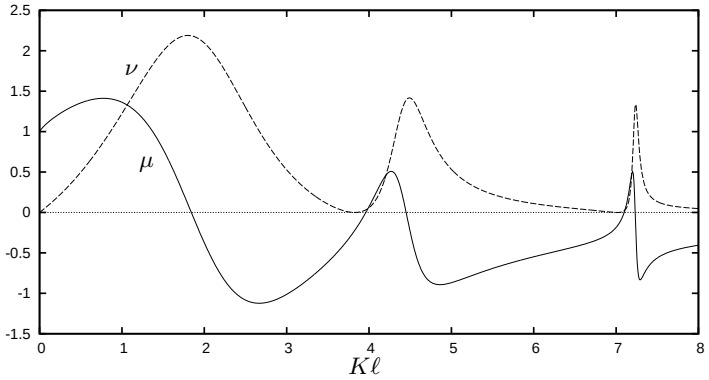

Figure 3. Dimensionless radiation conductance, μ, and radiation susceptance ν against $K\ell \equiv \omega^2\ell/g$ for the configuration in figure 4.

compared to its immersion depth; for smaller b/l, the variation of the coefficients around resonant frequencies (connected to zeros of Bessel functions) is much more pronounced and the first 'pumping mode' resonance can be more clearly identified and would be located much closer to its approximate value $K\ell \approx 1$, an asymptotic result based on $b/\ell \ll 1$, as described earlier.

In figure 4, we sketch out how the dimensionless capture width $\hat{l} = l/(L/2\pi)$, which cannot exceed unity according to this definition, varies with $K\ell$ for three different values of damping constant, $\hat{d}$. The dashed line in figure 3 represents the dimensionless maximum capture width, $\hat{l}_{max} \equiv l_{max}/(L/2\pi)$, given by (2.39), derived under the assumption λ real. The principal difference between the curves in figure 4 and figure 1 is that there are several peaks at which the maximum theoretical power can be absorbed and this is, as described in the previous section, directly associated with the multiple zeros of the susceptance, D. Thus each peak of $\hat{l}_{max} = 1$ occurs at the value of Kb at which $D = 0$ ($\mu = 0$).

The constant $\hat{d}$ which attains the capture width of $\hat{l} = 1$ at the first peak is given by matching $d = B$ at the frequency at which $D = 0$. This is $Kb \approx 1.84$ where $\nu \approx 2.18$ and then $\hat{d} = (K\ell)^{1/2}\nu \approx 1.05$, which is close to the value of $\hat{d} = 1$ used for one of the curves in figure 4. Interestingly, this value of $\hat{d}$ also appears to peak close to $\hat{l} = 1$ at subsequent frequencies, and this is related to the balance between the slow decay in the ν with the slow increase in $(K\ell)^{1/2}$ as Kb increases. Hence, the value of $\hat{d}$ needed to attain $\hat{l} = 1$ at the second peak is found to be $\hat{d} \approx 1.04$ and at the third peak $\hat{d} \approx 1.24$.

Otherwise, the curves of capture width in figure 4 show similar characteristics to those seen in figure 1 for the rigid-body motion in that for $\hat{d}$ greater much larger than the 'optimal value', $\hat{l}_{max}$ is never attained whilst, for $\hat{d}$ much less than this critical value, $\hat{l} = \hat{l}_{max}$ multiple times.

3. Examples of coupled resonant systems

The OWC example shows that it may be possible to exploit the intrinsic resonances to good advantage since the position of the zeros of the radiation susceptance varies

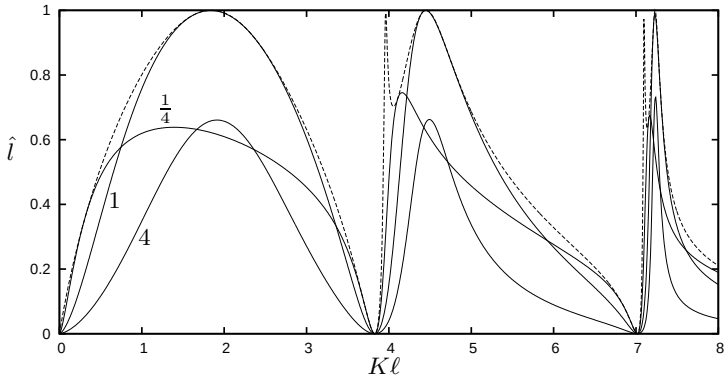

Figure 4. Curves showing the dimensionless capture width $\hat{l} = 2\pi l/L$ against $K\ell \equiv \omega^2\ell/g$ for a three-dimensional open-ended circular OWC device of radius-to-immersion depth $b/\ell = 8$ in water of finite depth, h where $\ell/h = \frac{1}{8}$ for three dimensionless damping constants, $\hat{d}$ (shown against curves). The dashed curve shows the maximum capture width $\hat{l} = \hat{l}_{max}$.

for example with the depth of submergence. In this section we look at a variety of WECs where we actively create coupled resonances.

(*a*) *Example: The Sperboy WEC device*

An interesting example of a WEC which exploits both rigid body resonance and oscillating water column resonances, as described in the previous section is the Sperboy WEC being developed by Embley Energy. This WEC is represented in its simplest form by a freely-floating thick-walled axi-symmetric cylinder with a hollow thin-walled tube extending to its lower open end below the cylinder and the upper end above the internal free surface connected in the usual way through a bi-directional air turbine.

Thus there are two resonances for this device configuration, one associated with the usual OWC resonance approximated by $\omega \approx \omega_1 = (g/\ell)^{1/2}$ where ℓ is the depth of the tube and the other associated with rigid-body motion at $\omega \approx \omega_2$ such that $M + A(\omega_2) - C/\omega_2^2 = 0$. In both resonances, there is differential motion between the internal free surface and the WEC structure resulting in power. The arguments above are based on ω_1 and ω_2 being spaced far enough apart that the resonances are essentially independent. In practice, they are coupled and the coupling effects can give rise to interesting power characteristics. The mathematical analysis of this device is complicated and not included here. Work by one of the authors for Embley Energy has shown that a broadbanded response can be achieved by suitably tuning the device geometry and turbine characteristics.

(*b*) *A coupled mass/spring/damper system*

As the first and simplest example we revisit the single mode rigid body motion case and instead of the device moving against a fixed reference, we shall assume that it drives a mass M_0, internal to the device, imparting a velocity U_0 to it. For example the heaving axisymmetric buoy or the pitching buoyant tethered cylinder

described in §2 may each contain the mass M_0. This case arises in the theory for the WEC PS Frog developed by Professor French and his colleagues at Lancaster University (French & Bracewell 1985).

The theory is similar to that for vibration dampers used to reduce large resonant oscillations of structures such as tall buildings. The idea is to the tune the new mass/spring system to the resonant frequency of the original mass thereby reducing large amplitudes of the latter. The method works but at the cost of introducing two new resonant frequencies either side of the original. Here we shall adapt the theory to a WEC device.

The external force on the device is now

$$X_e = -\lambda(U - U_0) \tag{3.1}$$

with $\lambda = d + \mathrm{i}\omega^{-1}\kappa$ as before, with d and κ positive spring and damping constants associated with the connection between the internal mass and the WEC. The equation of motion of the internal mass is

$$-\mathrm{i}\omega M_0 U_0 = \lambda(U - U_0)(= -X_e), \tag{3.2}$$

which we may re-write as

$$U_0 = \frac{\lambda(U - U_0)}{-\mathrm{i}\omega M_0}. \tag{3.3}$$

It follows from (2.3), and (3.1) that

$$X_s = \lambda(U - U_0) + UZ = (U - U_0)(\lambda + Z) + U_0 Z, \tag{3.4}$$

and substitution from (3.3) gives

$$(U - U_0)(\lambda(1 - Z/(\mathrm{i}\omega M_0)) + Z) = X_s, \tag{3.5}$$

or

$$(Z/Z_1)(U - U_0)(\lambda + Z_1) = X_s, \tag{3.6}$$

where

$$Z_1 = \frac{Z}{1 - Z/(\mathrm{i}\omega M_0)}. \tag{3.7}$$

Now the mean power absorbed is

$$W = -\tfrac{1}{2}\,\mathrm{Re}\{X_e\overline{(U - U_0)}\} = \tfrac{1}{4}(\lambda + \overline{\lambda})|U - U_0|^2, \tag{3.8}$$

which, using (3.6) becomes

$$W = \frac{|X_s|^2}{4|Z/Z_1|^2}\frac{\lambda + \overline{\lambda}}{|\lambda + Z_1|^2}. \tag{3.9}$$

Combining the relation (2.18) with Z_1 replacing Z, with $|Z/Z_1|^2\ \mathrm{Re}\{Z_1\} = \mathrm{Re}\{Z\} = B$ and using in (3.9) it follows that

$$W = \frac{|X_s|^2}{8B}\left(1 - \frac{|\lambda - \overline{Z_1}|^2}{|\lambda + Z_1|^2}\right), \tag{3.10}$$

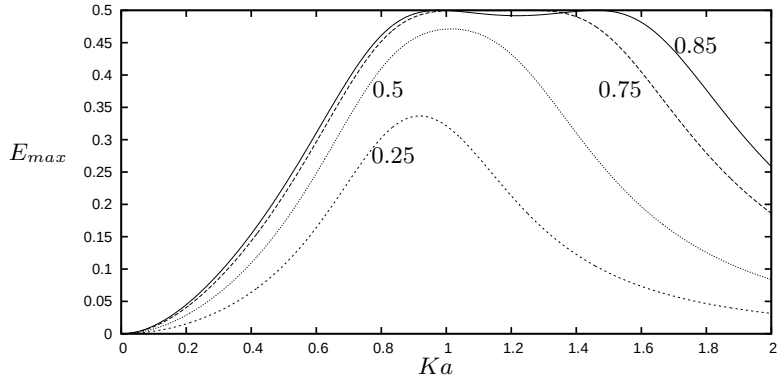

Figure 5. Curves showing maximum efficiency, E_{max}, against Ka for a semi-immersed horizontal cylindrical heaving buoy WEC, radius a, containing an internal mass M_0, zero spring restoring force and fixed dimensionless damping constants, $\hat{d} = 1$. The different curves show the proportional of mass assigned to the internal mass M_0/M_w where $M_w = \frac{1}{2}\rho\pi a^2$, varying from 0.25 to 0.85.

and again

$$W_{max} = \frac{|X_s|^2}{8B}, \tag{3.11}$$

achieved when $\lambda = \overline{Z_1}$, in agreement with (2.7). Efficiency (in two dimensions) or capture width (in three dimensions) can be calculated using (2.8) or (2.12).

It can be shown that the condition $\lambda = \overline{Z_1}$ for maximum power is the same as derived by Bracewell (1990) for the PS Frog WEC.

If λ is real then it can be shown, using (2.22), that

$$W_{max} = |X_s|^2/4(B + |Z|^2/|Z_1|), \tag{3.12}$$

although this result is of no practical use in this example where a non-zero spring restoring force is required for the internal mass.

(i) *A first illustrative example*

In figure 5 we return to the model of a two-dimensional semi-immersed cylinder constrained to move in heave only described in §2 *b*, but now taking power off through an internal mass/spring/damper mechanism. Curves show E_{max}, calculated via (3.12), for a system with zero spring constant when λ is real. This is physically unrealistic here, as a restoring force would be required for a mass contained internal to the cylinder. However, it provides a good illustration of the power absorption characteristics of such a device. The different curves all take a non-dimensional damping coefficient of $\hat{d} = 1$ and vary M_0/M_w where $M_w = \frac{1}{2}\rho\pi a^2$ is the total mass of the cylinder including the internal mass and $M + M_0 = M_w$ through Archimedes' principle. The results illustrate that for values of M_0/M_w less than 0.5, the maximum limit of $E = \frac{1}{2}$ is not attained at any frequency, but that as M_0/M_w is increased, E_{max} first peaks at $\frac{1}{2}$ before splitting into two distinct peaks separated by a broad plateau across which E_{max} maintains a high value.

In figure 6 we now take a fixed $M_0/M_w = \frac{3}{4}$ and $\hat{d} = \frac{1}{2}$ and vary the non-dimensional spring constant $\hat{\kappa} \equiv \kappa(a/g)/M_0$. When $\hat{\kappa} = 0$, the curve of efficiency

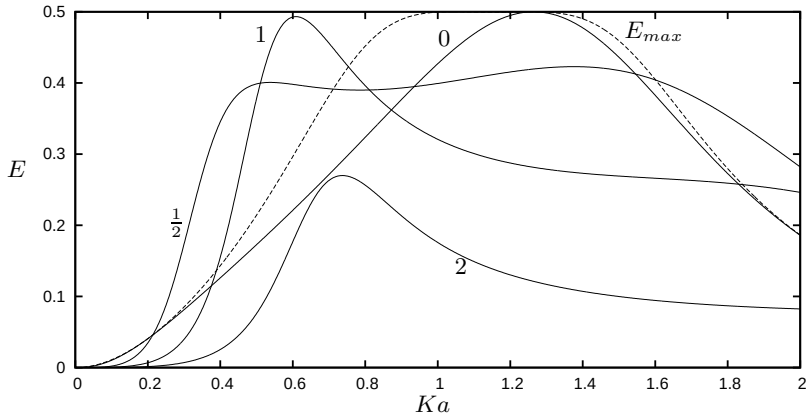

Figure 6. Curves efficiency, E, against Ka for a semi-immersed horizontal cylindrical heaving buoy WEC, radius a, containing an internal mass M_0, with internal mass $M_0/M_w = \frac{3}{4}$ and damping $\hat{d} = \frac{1}{2}$ fixed. The different curves represent different fixed values of spring constant $\hat{\kappa}$ (shown against curves). The maximum efficieny E_{max} for $\hat{\kappa} = 0$ is represented by the dashed curve.

calculated using (3.10) is contained under the curve of $E = E_{max}$, shown by the dashed curve. As $\hat{\kappa}$ is increased, results show how the efficiency varies as a function of Ka, by first plateauing with a high efficiency broad-banded response across a wide range of frequencies ($\hat{\kappa} = \frac{1}{2}$), then peaking ($\hat{\kappa} = 1$) and then falling away in efficiency as $\hat{\kappa}$ is increased further (e.g. $\hat{\kappa} = 2$). This latter behaviour is expected, since a stiff spring produces little relative motion between the cylinder and the internal mass, limiting the power absorption.

(ii) *A second illustrative example*

We now consider a two-dimensional problem of waves normally-incident on a submerged buoyant circular cylinder, which is tethered to the sea bed by inextensible mooring lines allowing free rotation of the cylinder axis about those mooring points on the sea bed. As the waves pass over the cylinder, it is forced into horizontal sway motion (under small-amplitude linearised theory) about the mean vertical position with the horizontal component of tension in the mooring lines providing a linear spring restoring force, C. Before setting up the coupled mass/spring/damper model, we return briefly to the simpler power absorption method described in §2 *b* by imagining that the cylinder is connected *externally* to a spring/damper system whose other end is attached to a fixed frame of reference. Then we may use all of the machinery developed in §2 *b* to determine the efficiency, using added mass and radiation damping coefficients for a submerged cylinder in sway in finite depth (see Evans & Porter (2007)) and with $C = M_w(1-s)g/\ell$ where M_w is the mass of the displaced water, $s = M/M_w$ is the ratio of the mass of the cylinder to that of the displaced water (i.e. the specific gravity) and ℓ is the length of the mooring line. As before, let us take $\kappa = 0$, so there is only a damper connection and sketch the results of maximum efficiency, E_{max}, see figure 7(a). In dimensionless form, Z equals $\nu - \mathrm{i}(s + \mu - (1-s)/Kl)$ and we recall that the maximum efficiency limit of $\frac{1}{2}$ for a symmetric cylinder is reached when $\mathrm{Im}\{Z\} = D = (s + \mu - (1-s)/Kl) = 0$.

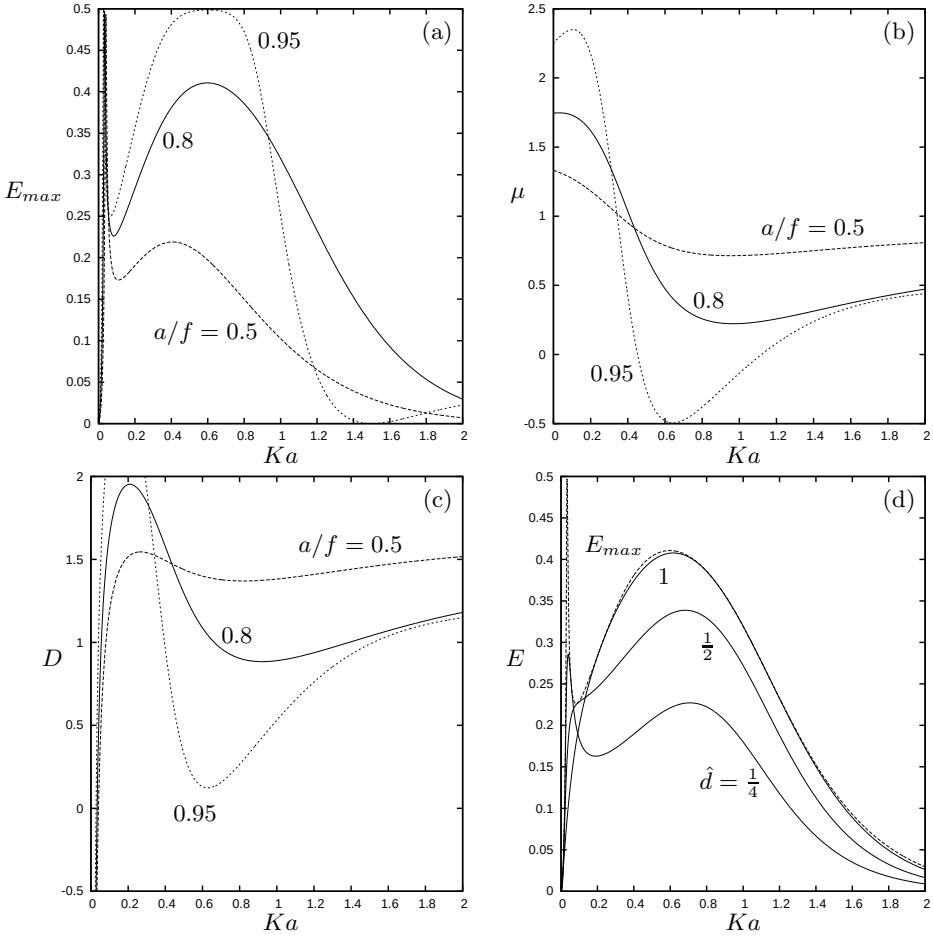

Figure 7. Various properties of a submerged buoyant cylindrical WEC of specific gravity $s = \frac{3}{4}$, tethered to the sea floor with $\ell/a = 3$, taking off power through a damper opposing sway motion. In (a), E_{max} for values of cylinder radius to submergence ratio a/f (shown against curves); (b) the corresponding variation in added mass; (c) the corresponding variation in D; (d) for $a/f = 0.8$, power extracted for different damping coefficients $\hat{d}$ (shown against solid curves) constrained by the maximum power E_{max} (dashed curve).

In the example considered in §2 *b* (i), D was zero only once. For this example, the situation is different and dependent on the ratio a/f where a is the cylinder radius and f the submergence of the cylinder axis below the surface. As shown in Evans & Porter (2007) the added mass, μ, drops below zero for a/f close to unity (a cylinder close to the surface) for small range of frequencies around $Ka = 1$, see figure 7(b). This phenomenon (explained by McIver & Falnes (1985)) allows D to approach zero again near $Ka = 0.6$ (see figure 7(c)) and two further zeros of D can occur for certain choices of a/f, s and ℓ/a.

The impact of these extra resonances (or near resonances) associated with $D = 0$ (or D close to zero) on the potential for power absorption is demonstrated in figure

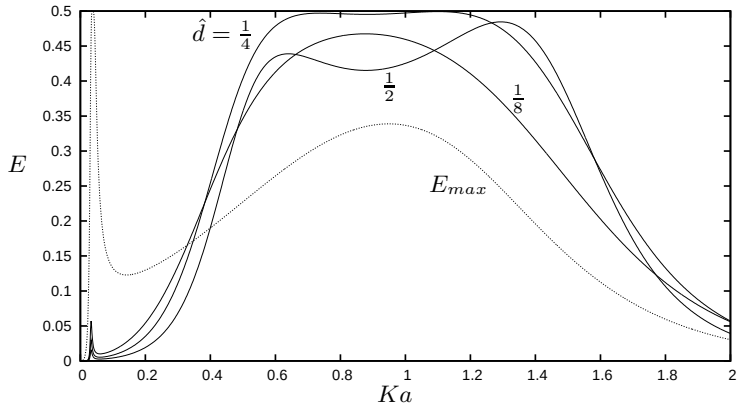

Figure 8. Curves of efficiency, E, against Ka for a submerged swaying tethered cylinder WEC, radius a, of mass M containing an internal mass M_0: $M/M_w = 0.15$, $M_0/M_w = 0.6$, $a/f = 0.8$ and $\ell/a = 3$. The spring constant is fixed at $\hat{\kappa} = \frac{1}{2}$ and different values of $\hat{d}$ are shown against curves. The dashed curve shows maximum efficiency in absence of a spring.

7(a) where, for $a/f = 0.95$, an additional high plateau in maximum efficiency, E_{max} close to the maximum of $\frac{1}{2}$, exists across a broad range of frequencies.

In figure 7(d) we take a less extreme value of $a/f = 0.8$, and show curves of power absorbed for three fixed damper values, $\hat{d}$, defined by $\hat{d} = d(a/g)^{1/2}/M_w$. It can be seen that the value of $\hat{d} = 1$ is optimal here.

In this section we are really interested in the effect of coupling structural resonances to an additional oscillating system. Thus, we now take the swaying cylinder example described above, remove the external damper and and insert an internal mass, M_0, inside the cylinder and connected to the cylinder by a spring and a damper, via which power is assumed to be absorbed. Now $s = (M_0 + M)/M_w$ is the specific gravity and we proceed as before, defining non-dimensional damping and spring constants with $\hat{d} = d(a/g)^{1/2}/M_0$, $\hat{\kappa} = \kappa(a/g)/M_0$ and using (3.10) with (3.7) and Z given by (2.4) to calculate the power and defining $E = W/W_{inc}$ as the efficiency, using (2.8).

In figure 8 we choose a set of parameters which mirror the curves shown in figure 7(d). That is, we choose $\ell/a = 3$ and $a/f = 0.8$ and, by setting $M/M_w = 0.15$ and $M_0/M_w = 0.6$, we retain the specific gravity of $s = \frac{3}{4}$. To illustrate the effectiveness of such a device, we have chosen a value of $\hat{\kappa} = \frac{1}{2}$ and varied the damping coefficient $\hat{d}$. It can be seen that the efficiency attains high values over a broad range of frequencies with $\hat{d} = \frac{1}{4}$ providing the best performance.

(c) *A WEC with projecting sidewalls*

The idea of building side-walls out from a WEC in order to create an additional resonance with the incident wave field was first proposed by Ambli *et al.* (1982) The aim is to first amplify the wave reaching the device through the organ pipe resonance created by the side walls. A simple approximate theory can be derived for the maximum power output which makes use of the two-dimensional performance of the device. Thus a wave of (complex) amplitude A travelling down the 'harbour' formed by the side-walls towards the device will be reflected as a wave of amplitude

Ar and re-reflected back down the harbour with amplitude ArR where r, R are the reflection coefficients of the device at the open end respectively. This process, when repeated indefinitely, ultimately gives rise to a wave of amplitude $A/(1-rR)$ travelling towards the device and $Ar/(1-rR)$ travelling away from it. It follows that the capture width ratio based on the distance $2b$ between the side-walls for incident waves travelling parallel to the side-walls, is the difference between incoming and outgoing wave energy, namely

$$l/2b = (1-|r|^2)/|1-rR|^2, \tag{3.13}$$

which may be written

$$l/2b = \frac{1}{1-|R|^2}\left(1-\frac{|r-\overline{R}|^2}{|1-rR|^2}\right), \tag{3.14}$$

so that when $r=\overline{R}$,

$$l_{max}/2b = \frac{1}{1-|R|^2}. \tag{3.15}$$

If we now take $|R| = \mathrm{e}^{-kb}$ (Noble 1958), where $K = k\tanh kh$ and h is the depth of the fluid, being the result for plane waves travelling towards the open end of a semi-infinite duct, we see that

$$l_{max}/2b = (1-\mathrm{e}^{-2kb})^{-1} \tag{3.16}$$

as the maximum capture width of an isolated device with projecting side-walls. Here $k=2\pi/L$ where L is the wavelength. Notice that in long waves, $l_{max}\sim k^{-1} = L/2\pi$ as $kb\to 0$, the result for a point absorber, whilst in short waves, $l_{max}\sim 2b$.

If the WEC is positioned the middle of a narrow wave tank of width $2a$, the reflection coefficient R for waves travelling along and towards the open end of a semi-infinite duct of width $2b$ ($b<a$) is needed. Thus it can be shown that $|R| = 1-b/a$ so that the maximum efficiency of a device with side-walls of width $2b$ operating in the middle of a wave tank of width $2a$ is simply

$$E_{max} = (2-b/a)^{-1}. \tag{3.17}$$

It follows that $E_{max}\to\frac{1}{2}$ as $b/a\to 0$ in agreement with Srokosz (1980) for point absorbers in channels, whereas $E_{max}\to 1$ as $b/a\to 1$ since in this case the device spans the entire width of the tank.

The same multiple-reflection arguments can be used to derive an expression for the capture width ratio in terms of λ the power take-off characteristic, Z, the two-dimensional impedance term given by (2.4), and r_0, the two-dimensional reflection coefficient for the device assumed to be fixed at the end of a semi-infinite duct. Thus

$$\frac{l}{2b} = \frac{|\lambda+Z|^2-|\lambda-\overline{Z}|^2}{|(\lambda+Z)-r_0R(\lambda-\overline{Z})|^2} \tag{3.18}$$

obtained by using the relation

$$Z^h = \frac{Z+r_0R\overline{Z}}{1-r_0R} \tag{3.19}$$

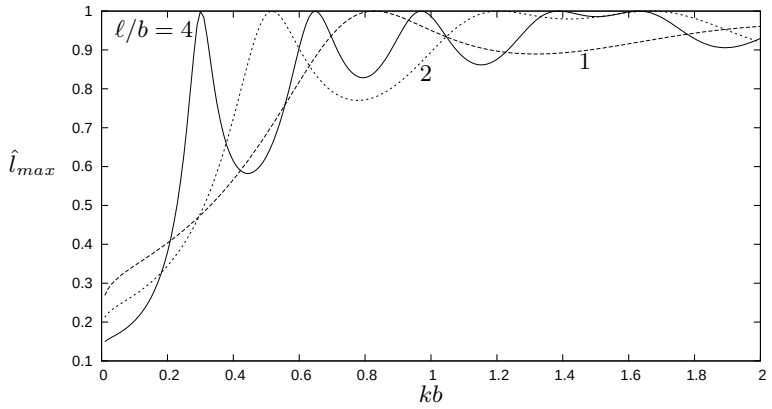

Figure 9. Curves of non-dimensional maximum capture width $\hat{l}_{max}$ against kb for piston absorber a distance ℓ along a duct of width $2b$, when operating with real λ, for different different values of ℓ/b (shown against curves).

This can be re-arranged into the form

$$\frac{l}{2b} = \frac{1}{1-|R|^2}\left(1 - \frac{|\lambda - \overline{Z^h}|^2}{|\lambda + Z^h|^2}\right) \tag{3.20}$$

confirming the result (3.15) when $\lambda = \overline{Z^h}$. If λ is restricted to be real then we obtain

$$\frac{l_{max}}{2b} = \frac{1}{(1-|R|^2)}\frac{2B^h}{|Z^h| + B^h} \tag{3.21}$$

where $B^h = \mathrm{Re}\{Z^h\} \equiv B(1-|R|^2)/|1-r_0R|^2$. Results can be found in Count & Evans (1984) where it is shown (figure 7 of that paper) that as the length of the side-walls increases the performance is improved markedly over a range of frequencies.

(i) *Illustrative results*

As already demonstrated, with reference to (3.15), (3.16), the maximum theoretical capture width for a device without sidewalls can be amplified by adding sidewalls. For the purposes of presentation, we define a scaled dimensionless capture width $\hat{l} = (1-|R|^2)l/2b$ so that $\hat{l}$ cannot exceed unity. We return to the example considered by Count & Evans (1984), of a piston wave absorber of width $2b$ and height h operating between parallel walls separated by $2b$ and at a distance a along the duct from the opening. Here, $r_0 = 1$, the reflection coefficient from a vertical fixed wall. The depth of the water is h. There is no natural restoring force for such a wave absorber and so $C = 0$ and $Z = B - \mathrm{i}\omega(M + A)$, where B and A are the added mass and damping for the piston wave absorber in motion in a semi-infinite duct and $M = 2\rho bhd$ is the mass of the wave absorber where d is the depth of the absorber. Thus, the non-dimensional Z is $\nu - \mathrm{i}(d/h + \mu)$ where $\nu = B/(2\rho bh^2\omega)$ and $\mu = A/(2\rho bh^2)$. In figure 9 we show the effect of varying the length of the duct, ℓ/b, when $d/h = 0.1$, $b/h = 1$ are fixed, as a function of kb, where $K = k\tanh kh$. Curves in figure 9 show the maximum dimensionless capture width in the case of real λ (i.e.

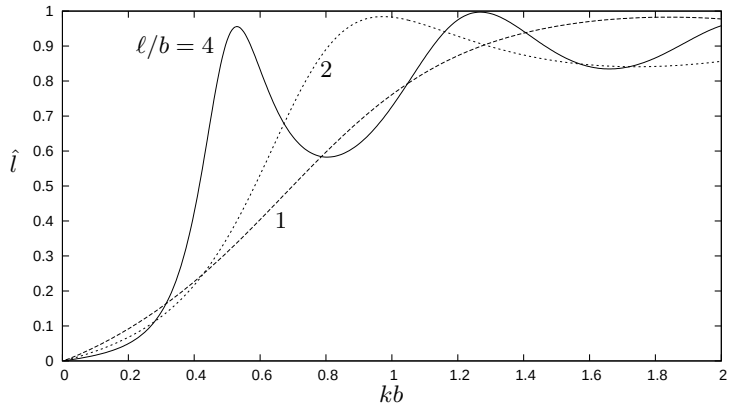

Figure 10. Curves of non-dimensional capture width $\hat{l}$ against kb for piston absorber a distance ℓ along a duct of width $2b$, when operating with fixed damper and spring constants $\hat{d} = 1$, $\hat{\kappa} = \frac{1}{2}$. Values of ℓ/b shown against curves.

no spring force attached to the absorber), and demonstrate an increasing number of peaks to the maximum value of unity as the length of the duct is increased, associated with 'duct resonances'. In practice for such a WEC, a spring is required to provide a restoring force. Thus, in figure 10 we show curves of dimensionless capture width for fixed damper and spring constants, $\hat{d} = 1$ and $\hat{\kappa} = 1$, defined by $\hat{d} \equiv d/(2\rho h^2(bg)^{1/2})$ and $\hat{\kappa} = \kappa/(2\rho h^2 g)$ for the same parameters as shown in figure 9.

(*d*) *A WEC containing an internal water tank*

In this section we assume the WEC is of the type described by the second example in the rigid body part of §2. Specifically it is a totally submerged, buoyant cylinder tethered to the sea-bed by inextensible mooring lines with its axis horizontal, and making small oscillations in pitch due to the horizontal component of the tension in the moorings due to its buoyancy. Furthermore the WEC is assumed to be symmetric about a vertical plane through its centre, and encloses a body of water with a free surface so that it is free to move in response to the motion of the WEC. The use of a water tank to reduce unwanted motions of structures is well-known and an extensive theory exists for what are termed tuned liquid dampers. See for example Ibrahim (2009). Here we shall consider their role in the context of WECs and coupled resonances.

In the absence of any damping of the enclosed water the effect of the tank is simply to exert an external force on the WEC in the form of

$$X_e = \mathrm{i}\omega A_u U \tag{3.22}$$

where A_u is the added mass of the enclosed water, dependent on frequency. This clearly cannot contribute to any power absorption by the WEC but can affect the motion appreciably if the lowest sloshing frequency coincides with the resonant frequency of the WEC.

In order to extract power from the system we have to introduce damping. One way of doing this is as follows. For simplicity we assume the incident wave crests

are parallel to the generatrices of the cylinder so that all motions take place in an (x, y)-plane and are antisymmetric about $x = 0$. We assume the free surface of the enclosed water to occupy $-c < x < c$ and that the air trapped above the free surface in $0 < x < c$ is forced by the antisymmetric motion to pass into the region $-c < x < 0$ above the free surface by way of a turbine contained in a thin rigid baffle extending from the roof of the tank to just below the free surface. Thus the pressure on the free surface, in excess of atmospheric will be P and $-P$ in $0 < x < c$ and $-c < x < 0$ respectively.

On the basis of linear water wave theory, there exists a velocity potential governing the sloshing of fluid in the tank contained in the WEC given by Φ which is harmonic and satisfies

$$\Phi(x, y) = -\Phi(-x, y) \tag{3.23}$$

so that we need only consider $0 < x < c$ provided we ensure that

$$\Phi(0, y) = 0. \tag{3.24}$$

We also require

$$\Phi_n = U n_x, \tag{3.25}$$

on S, the internal surface of the WEC bounding the enclosed water in $x > 0$, where n_x is the horizontal component of the normal to S and the subscript n denotes the normal derivative to S. On the free surface, $y = 0$, (see for example, Evans (1982)), it can be shown that we have

$$K\Phi - \Phi_y = -\mathrm{i}\omega P/\rho g, \qquad 0 < x < c. \tag{3.26}$$

It is convenient to write

$$\Phi = U\phi^{(u)} + P\phi^{(p)}, \tag{3.27}$$

where $\phi^{(u)}$ satisfies (3.24), and (3.25) with $U = 1$, and (3.26) with $P = 0$, whilst $\phi^{(p)}$ satisfies (3.24), (3.25) with $U = 0$, and (3.26) with $P = 1$. It follows that $\phi^{(u)}$ is real and $\phi^{(p)}$ is pure imaginary. The external force is now

$$X_e = 2\mathrm{i}\omega\rho \int_S \Phi(x, y) n_x \mathrm{d}s \equiv U f_u + P f_p, \tag{3.28}$$

where

$$f_{u,p} = 2\mathrm{i}\omega\rho \int_S \phi^{(u,p)}(x, y) n_x \mathrm{d}s, \tag{3.29}$$

and the factor of 2 arises since $\phi^{(u)}$ is odd in x and S accounts for only one half of the total symmetrical tank wetted surface.

Thus f_p is real and f_u is pure imaginary so that we write $f_u = \mathrm{i}\omega A_u$, with A_u real. The volume flux (per unit length) across the free surface in $(0, c)$ is

$$Q = \int_0^c \Phi_y(x, 0)\mathrm{d}x = (U q_u + P q_p), \tag{3.30}$$

where we define

$$q_{u,p} = \int_0^c \phi_y^{(u,p)}(x, 0)\mathrm{d}x. \tag{3.31}$$

Hence q_u is real and q_p is pure imaginary so that we write $q_p = \mathrm{i}\omega A_p$, with A_p real. The air turbine characteristics are modelled by a constant λ linking the volume flux through the air turbine to the pressure across it via a linear damping law, as described in §2 *c*. Thus we assume

$$Q = 2\lambda P, \tag{3.32}$$

the factor of two arising since the difference in pressure across the air turbine equates to $2P$ here. It follows from (2.3) and (3.28) that

$$Z_1 U = P f_p + X_s, \qquad \text{where } Z_1 = Z - \mathrm{i}\omega A_u, \tag{3.33}$$

whilst from (3.30) and (3.32),

$$U q_u = (2\lambda - \mathrm{i}\omega A_p) P. \tag{3.34}$$

It follows from (3.34) that we may write (3.34) as

$$\frac{2Z_1}{q_u}\,(\lambda + Z_2)\,P = X_s, \tag{3.35}$$

where

$$Z_2 = q_u^2/Z_1 - \tfrac{1}{2}\mathrm{i}\omega A_p, \tag{3.36}$$

and we have used the result

$$f_p = -2q_u, \tag{3.37}$$

which can be proved by a simple application of Green's second identity to $\phi^{(u)}$ and $\phi^{(p)}$ in the domain $x \geq 0$ occupied by the fluid.

Now the mean power absorbed for this system is

$$W = \mathrm{Re}\{Q\overline{P}\} = (\lambda + \overline{\lambda})|P|^2, \tag{3.38}$$

where, for the moment, we have assumed that λ is complex so that, from (3.35),

$$W = \frac{1}{4}\frac{(\lambda + \overline{\lambda}) q_u^2 |X_s|^2}{|Z_1|^2 |\lambda + Z_2|^2}. \tag{3.39}$$

Using the result (2.18) with Z_2 replacing Z and the relation $|Z_1|^2\,\mathrm{Re}\{Z_2\} = q_u^2 B$ allows us to express the power as

$$W = \frac{|X_s|^2}{8B}\left(1 - \frac{|\lambda - \overline{Z}_2|^2}{|\lambda + Z_2|^2}\right) \tag{3.40}$$

and the maximum power, achieved when $\lambda = \overline{Z_2}$, is in agreement with (2.7). However, if air compressibility is neglected, then λ is real in which case we return to (3.39) and use the identity (2.22) with Z_2 replacing Z. Now, for real λ,

$$W_{max} = \frac{1}{4}\frac{q_u^2 |X_s|^2}{|Z_1^2|(|Z_2| + \mathrm{Re}\{Z_2\})} \tag{3.41}$$

which may be written

$$W_{max} = \frac{1}{4}\frac{|X_s|^2}{(B + |Z_1||1 - \frac{1}{2}\mathrm{i}\omega A_p Z_1/q_u^2|)} \tag{3.42}$$

and is achieved when $\lambda = |Z_2|$.

(i) *An example: a tank of rectangular cross-section*

We consider solving for the potentials $\phi^{(u)}$ and $\phi^{(p)}$ in the special case of a WEC encasing a tank of rectangular cross-section containing water in $-d < y < 0, -c < x < c$. We first consider the possible modes of oscillation of the water in the WEC when it is at rest. Separation of variables gives two sets of modes, odd and even about the centreline $x = 0$. For the odd modes, which are the only ones which concern us here, separation solutions are given by

$$\sin p_n x \cosh p_n(y+d), \quad p_n = (n - \tfrac{1}{2})\pi/c, \qquad n = 1, 2, \ldots \tag{3.43}$$

where the eigenfrequencies $\omega = \omega_n$ are determined by application of the homogeneous free surface condition as

$$p_n \tanh p_n d \equiv \omega_n^2/g. \tag{3.44}$$

When the WEC is in motion, the potential is split according to (3.27). We require $\phi^{(u,p)}$ to be harmonic in $0 < x < c$, $-d < y < 0$ and satisfy

$$\phi^{(u,p)}(0, y) = 0, \qquad -d < y < 0, \tag{3.45}$$

$$\phi^{(u,p)}_y(x, d) = 0, \qquad 0 < x < c, \tag{3.46}$$

$$\phi^{(u,p)}_x(c, y) = (1, 0), \qquad -d < y < 0, \tag{3.47}$$

$$K\phi^{(u,p)}(x, 0) - \phi^{(u,p)}_y(x, 0) = (0, -\mathrm{i}\omega/\rho g), \qquad 0 < x < c, \tag{3.48}$$

where $K = \omega^2/g$ as usual. If we let

$$\phi^{(u)} = x + \phi^{(0)}, \tag{3.49}$$

then $\phi^{(0)}$ satisfies all the above conditions on $\phi^{(u)}$ except on the free surface where

$$K\phi^{(0)}(x, 0) - \phi^{(0)}_y(x, 0) = -Kx, \qquad 0 < x < c. \tag{3.50}$$

We may Fourier-expand both $\phi^{(0)}$ and $\phi^{(p)}$ in terms of the modes defined in (3.43)

$$\phi^{(0,p)}(x, y) = \sum_{n=1}^{\infty} \frac{B_n^{(0,p)} \cosh p_n(y+d) \sin p_n x}{(p_n \sinh p_n d - K \cosh p_n d)}, \tag{3.51}$$

which satisfies all conditions except on the free surface, requiring

$$\sum_{n=1}^{\infty} B_n^{(0,p)} \sin p_n x = (Kx, \mathrm{i}\omega/\rho g), \qquad 0 < x < c. \tag{3.52}$$

Thus we find that

$$B_n^{(0,p)} = \left(-2K(-1)^n/(p_n^2 c), 2\mathrm{i}\omega/(g\rho p_n c)\right). \tag{3.53}$$

It follows from (3.29) that

$$f_{u,p} = 2\mathrm{i}\omega\rho \int_{-d}^{0} \phi^{(u,p)}(c, y)\mathrm{d}y = 2\mathrm{i}\omega\rho \left(cd(1, 0) - \sum_{n=1}^{\infty} \frac{B_n^{(0,p)}(-1)^n \omega_n^2}{p_n^2(\omega_n^2 - \omega^2)} \right) \tag{3.54}$$

where the identity

$$\frac{\sinh p_n d}{p_n \sinh p_n d - K \cosh p_n d} = \frac{\omega_n^2}{p_n(\omega_n^2 - \omega^2)} \tag{3.55}$$

has been used. Thus $f_u = \mathrm{i}\omega A_u$ where A_u, the added mass of the sloshing water is

$$A_u = M_t \left(1 + \frac{2\omega^2 c^2}{gd} \sum_{n=1}^{\infty} \frac{\omega_n^2}{(p_n c)^4(\omega_n^2 - \omega^2)} \right) \tag{3.56}$$

where $M_t = 2\rho cd$ is the mass of water per unit length in the WEC. Thus, the added mass tends to the mass of the water when the frequency tends to zero as expected. We also have, from (3.31),

$$q_{u,p} = \int_0^c \phi_y^{(u,p)}(x,0)\mathrm{d}x = \int_0^c \phi_y^{(0,p)}(x,0)\mathrm{d}x = \sum_{n=1}^{\infty} \frac{B_n^{(0,p)} \omega_n^2}{p_n(\omega_n^2 - \omega^2)}. \tag{3.57}$$

It follows from (3.53), (3.54) that

$$f_p = 4Kc^2 \sum_{n=1}^{\infty} \frac{(-1)^n \omega_n^2}{(p_n c)^3(\omega_n^2 - \omega^2)} = -2q_u, \tag{3.58}$$

as predicted in (3.37). We also have, from (3.53), (3.57) with $q_p = \mathrm{i}\omega A_p$,

$$A_p = \frac{2c}{\rho g} \sum_{n=1}^{\infty} \frac{\omega_n^2}{(p_n c)^2(\omega_n^2 - \omega^2)}. \tag{3.59}$$

(ii) *Results*

We return to the configuration used earlier in §3 *b* (ii), of a buoyant tethered circular cylinder WEC, which is now assumed to incorporate an internal water tank of rectangular cross-section, as described above. Power is taken off through a bi-directional turbine placed in a barrier dividing the airspace above the internal free surface into two equal halves. When in motion, incident waves force the submerged cylinder to pitch about the fixed axis of rotation on the sea floor and this drives the motion in the internal water tank which drives the air through the turbine. The idea is to couple the resonant motion of the WEC with the resonant motion of the internal sloshing modes (of which the fundamental mode is the most important).

We stick to the main parameters used to illustrate the internal spring/mass/damper system used in §3 *b* (ii). That is, the cylinder radius, a is related to the depth of submergence of the cylinder by $a/f = 0.8$; the length of the tether ℓ is fixed at $\ell/a = 3$; the mass of the cylinder (excluding internal water) is $M/M_w \equiv M/(\frac{1}{2}\rho\pi a^2) = 0.15$.

Initially, we aim to show results for an internal tank of realistic physical dimensions, that is, the tank fits within the WEC. In figure 11, curves show $c/d = 4, 3, 2$ and fix $c/a = 0.99, 0.986, 0.942$ (respectively) to ensure the fit. By increasing aspect ratio c/d and allowing c/a to be as large as possible, we are able to lower the natural frequencies of oscillation of the internal water tank, in the cases described to the equivalent of $Ka = 0.59$, 0.76 1.09 (respectively). The effect of these natural frequencies is apparent in the results of figure 11. In the left-hand panel of

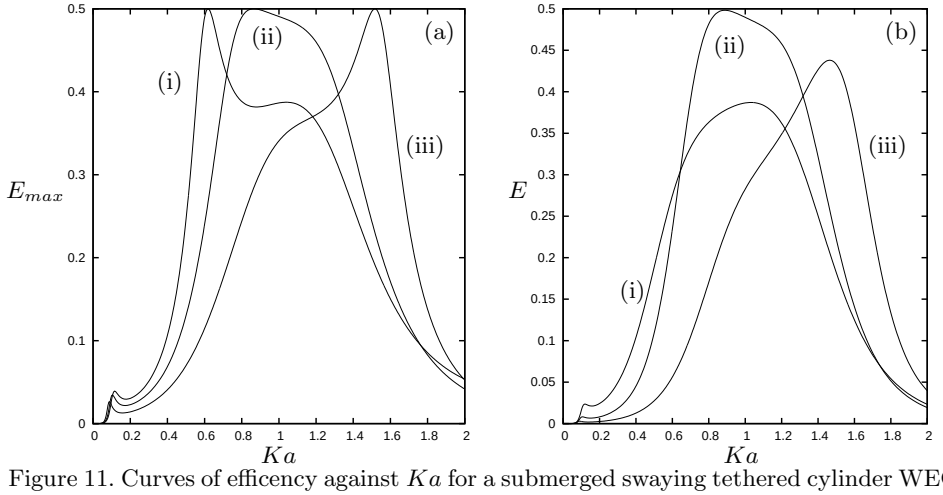

Figure 11. Curves of efficency against Ka for a submerged swaying tethered cylinder WEC, radius a, with an internal water tank. Here, $a/f = 0.8$, $M/M_w = 0.15$ and $\ell/a = 3$ whilst curves show: (i) $c/d = 4$, $c/a = 0.99$; (ii) $c/d = 3$, $c/a = 0.984$; (iii) $c/d = 2$, $c/a = 0.942$. In (a), E_{max} is shown for optimal real λ and, in (b), E is shown for a fixed real λ ($\hat{\lambda} = 10$).

figure 11, we sketch curves of E_{max}, the maximum efficiency for real power-take of parameter, λ, as given by (3.42), with $E_{max} = W_{max}/W_{inc}$ and W_{inc} defined by (2.8). In the right-hand panel is shown corresponding curves for fixed real λ, with $\hat{\lambda} = 10$ and $\hat{\lambda} = \lambda M_w g^{1/2}/c^{5/2}$. Thus, curves in figure 11(b) are bounded above by the corresponding curves in figure 11(a). We observe the characteristics of coupled resonances in that single peaks in efficiency are replaced by more complicated plateau-type behaviour with peaks related to the fundamental sloshing frequencies in the internal tank. In the case of $c/d = 3$ with $c/a = 0.984$ we see efficiency close to the limit of $\frac{1}{2}$ over a broad range of frequencies.

In the example covered here, we have assumed a rather simple configuration for the internal water tank. In particular, the mechanisms for controlling the natural frequencies of oscillation have been restricted by the tank geometry. Introducing a more complicated tank configuration will allow us to alter those natural frequencies more readily and we might expect other interesting effects to be observed. As an indication of these effects, we now include an 'artificial' tank which cannot be physically confined within the circular WEC device.

In figure 12 we show a cylinder configuration from before but with $c/d = 1.5$ and $c/a = 3$ in the left-hand panel and $c/d = 3$ with $c/a = 5$ in the right-hand panel. The figures show both the optimal E_{max} for λ real and E for a fixed value of λ, set at $\hat{\lambda} = 1.5$ and 0.15 in the two figures. In the left-hand panel, we observe that the plateau has been broadened and shifted to lower values of Ka as the fundamental sloshing frequency in the tank is lowered to $Ka = 0.5$. In the right-hand panel, the curve of E_{max} now contains a number of peaks close to the maximum value of 1/2. Here, the tank is wide and shallow and the fundamental sloshing frequency is located at an even lower value of $Ka = 0.23$, whilst the effect of the second-order sloshing mode is now apparent occurring at $Ka = 1.73$.

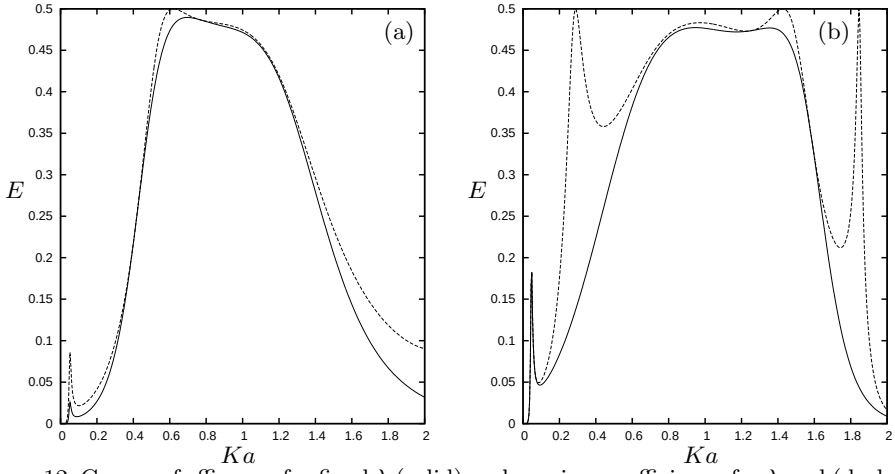

Figure 12. Curves of efficency for fixed λ (solid) and maximum efficiency for λ real (dashed) against Ka for a submerged swaying tethered cylinder WEC, radius a, with an internal water tank with the same parameters as in figure 11, apart from: (a) $c/d = 3$, $c/a = 1.5$; (b) $c/d = 5$, $c/a = 2$.

4. A new concept: the ROTA WEC

We develop the theme introduced at the end of the previous section and outline a new concept for a WEC based on coupled resonant systems. Instead of taking power out of an internal water tank by driving air above two separate air chambers through a bi-directional turbine, a much simpler, more efficient and robust power take off mechanism is considered. Thus, we envisage an internal tank which is free to develop lateral sloshing motions in response to wave forcing. At resonance, which is determined by a fully coupled model, the predicted large amplitude response in the motion of water in the internal tank will feed water via shaped walls into an internal reservoir whose purpose is to control the storage of a head of water and release this water back into the main tank of water via a low-head turbine from which electricity is generated. The WEC concept is called ROTA and is an acronym for *Resonant Over-Topping Absorber* and its proposed design is shown in figure 13.

Current thinking envisages the ROTA to consist of a submerged buoyant circular cylinder having a length roughly four times its diameter of between 10 and 15 metres (eventual shape and dimensions will be decided on the basis of information gained during any subsequent research and any further tank or field tests). The cylinder is held under tension with its axis horizontal and at right angles to the predominant direction of the incident wave field, by inextensible mooring lines (A) attached at each end and connected to the seabed. Adjustments to buoyancy (F), the length of the mooring lines, the shape of the tank walls and the depth of submergence of the cylinder determine conditions for resonance. In turn, the predominant sway motion of the cylinder creates a sloshing motion in the enclosed water in the chamber causing it to run up the internal sides of the chamber which are shaped to assist overtopping of the water through the air space (G) into the inner reservoir (D) which extends along the length of the chamber (in practice, it would be separated by baffles into separate chambers to mitigate against transverse sloshing). The inner

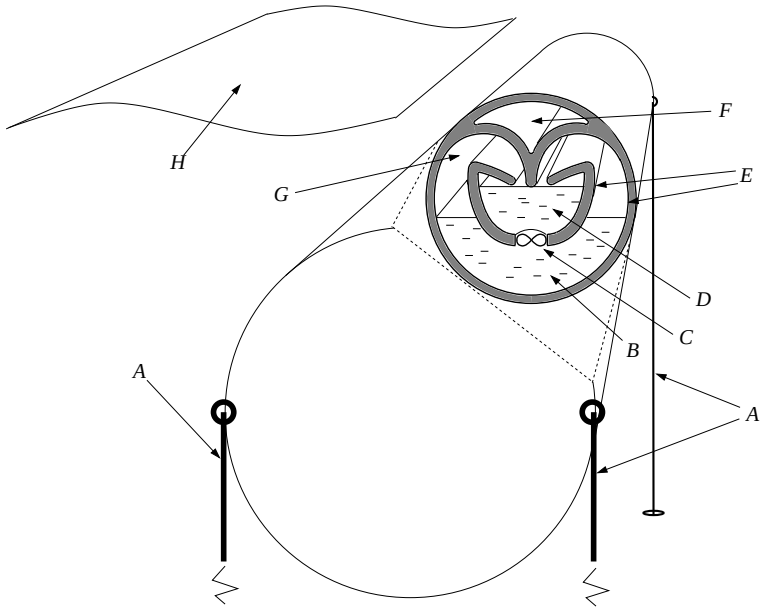

Figure 13. Schematic drawing of the proposed ROTA WEC device.

reservoir extends above the equilibrium position of the enclosed water (B) so that a differential head of water is built up and maintained by controlling its release into the main body of the water in the chamber through the low-head turbine (C) from which electricity is generated.

Although there are some aspects of the ROTA which are not advantageous to the device operation (tidal variation, exposure to currents, maintenance) there are also key advantages of the ROTA over some other existing WEC designs. These include:

(i) Because the device is totally submerged, it is protected from the effect of severe seas and corresponding wave forces.

(ii) Securing the structure to the sea bed provides a fixed frame of reference against which it can operate whilst allowing it to move with the waves, again reducing excessive wave forces.

(iii) A careful choice of design parameters to achieve resonance ensures an optimal transfer of energy from the waves first to the sides of the structure and then into the inner reservoir.

(iv) Theory suggests (Evans 1980) and experiments confirm that a submerged device absorbing energy through a horizontal motion in the direction of the incident waves has the potential for absorbing more energy than a device absorbing energy from moving vertically.

(v) The device has few moving mechanical parts and uses a well-established power take-off technology.

(vi) The mooring system permits rotatory motion only thus avoiding the end-stop problem associated with linear translatory motions such as heave.

The success in creating a broad-band high power absorption response in the final example of §3, which is closely related to the ROTA WEC provides a good indication of the potential for success of this concept. Such a WEC, which relies on large amplitude motions to generate overtopping for successful operation will require small-scale testing and numerical simulations to fully realise its potential.

5. Conclusion

In this paper we have described a range of different wave energy absorbers and the mathematical theories that underpin them. Classical linearised water wave theory is used in each setting to develop expressions for the power absorption for a particular power take-off mechanism, and the maximum theoretical power absorption.

We start with a review of established results for power take-off from rigid bodies and oscillating water columns constrained to operate in a single degree of freedom and illustrate typical results for efficiency and capture width of such devices. The role that resonance plays in optimising power absorption is highlighted in the examples that are give. The focus thereafter is on introducing systems which display multiple resonances and, in each example given in the paper, this is shown to assist in broadening the range of frequencies over which significant power can be absorbed. Such multiple resonances can be built into a system in two ways. A WEC may be designed to exhibit resonance through a single mode of operation but at more than one frequency, as in the examples of OWC devices or devices with sidewalls. Alternatively it can be manufactured by coupling systems each with their own resonant frequencies in such a way that the overall performance is enhanced. Currently devices such as the Sperboy WEC and the PS Frog are designed with coupled systems in place, and systems closely related to the PS Frog operation are investigated in § *b* of the paper in which a rigid body motion, forced by incident waves, is coupled to an internal mass/spring/damper system.

Finally, we look at creating a coupled resonant system capable of taking power from the waves when an internal water tank is placed inside a WEC device. Specifically, we focus results on a submerged buoyant tethered circular cylinder which incorporates a rectangular tank of water whose sloshing motion is used to generate power via an air turbine placed above the internal free surface of the tank. Here, we are able to show some promising initial results which demonstrate that a significant power can be absorbed over a range of realistic wave frequencies via a suitable tuning of various parameters.

The results from last part of section 3 leads us to speculate that a new device called the ROTA could emerge as having the potential to be a successful WEC. Not only is its design built on a strong theoretical footing, but the concept has considered carefully many of the engineering challenges that confront wave energy production.

References

Ambli, N., Bonke, K., Malmo, O. & Reitan, A. 1982, The Kvaerner Multiresonant

OWC. In *Proc. 2nd Intl. Symp. on Wave Energy Utilization, Trondheim, Norway.*, pp. 275–297.

Bracewell, R. H. 1990 *A study of two reactionless ocean wave energy converters.* Ph.D. Thesis, Lancaster University.

Budal, K. & Falnes, J. 1975 A resonant point absorber of ocean-wave power. *Nature,* **256**, 478–479; corrigendum **257**, p.626.

Count, B. M. & Evans, D. V. 1984 The influence of projecting sidewalls on the hydrodynamic performance of wave energy devices. *J. Fluid Mech.* **145**, 361–376.

Cruz, J. (ed.) 2008 *Ocean Wave Energy: Current Status and Future Prespectives.* Springer.

Evans, D. V. 1976 A theory for wave-power absorption by oscillating bodies. *J. Fluid Mech.* **77**, 1–25.

Evans, D. V. 1980 Some analytical results for two and three dimensional wave-energy absorbers. In *Power from Sea Waves* (ed. B. Count) pp. 213–249.

Evans, D. V. 1982 Wave-power absorption by systems of oscillating surface pressure distributions. *J. Fluid Mech.* **114** 481–499.

Evans, D. V., Jeffrey, D. C., Salter, S. H. & Taylor, J. R. M. 1979 Submerged cylinder wave-energy device: theory and experiment. *Appl. Ocean Res.* **1**, 3–12.

Evans, D. V. & Porter, R. 1995 Hydrodynamic characteristics of an oscillating water column device. *Appl. Ocean Res.* **17**(3), 155–164.

Evans, D. V. & Porter, R. 2007 Wave free motions of isolated bodies and the existence of motion trapped modes. *J. Fluid Mech.* **584**, 225–234.

Falcão, A F de O. 2010 Wave energy utilization: A review of the technologies. *Renewable & Sustainable Energy Rev.* **14**, 889–918.

Falnes, J. 2002 *Ocean Waves and Oscillating Systems.* Cambridge University Press.

Falnes, J. & McIver, P. 1985 Surface wave interactions with systems of oscillating bodies and pressure distributions. *Appl. Ocean Res.* **7**(4), 225–234.

French, M. J. & Bracewell, R. H. 1985 Heaving point absorbers reacting against an internal mass. In *Hydrodyn. Ocean Wave Energy Util. IUTAM Symp. Lisbon. 1985*, Berlin/Heidelberg: Springer pp. 247–255.

Martin, P. A. & Dixon, A. G. 1983 The scattering of regular surface waves by a fixed, half-immersed, circular cylinder. *Appl. Ocean Res.* **5**(1), 13–23.

Mei, C. C. 1976 Power extraction from water waves. *J. Ship Res.* **20**, 63–66.

Newman, J. N. 1976 The interaction of stationary vessels with regular waves. In *11th Proc. Symp. Naval Hydrodyn., London*, pp. 491–501.

Salter, S. H. 1974 Wave power. *Nature*, **249**, 720–724.

Srokosz, M. A. 1980 Some relations for bodies in a canal, with an application to wave power absorption. *J. Fluid Mech.* **99**, 145–162.